Supplementary information

Facile synthesis of Au@Fe_3O_4-graphene and Pt@Fe_3O_4-graphene ternary hybrid nanomaterials and their catalytic properties

Baoping Lu [a, b], Zhe Zhang [a], Jinhui Hao [a, b], Jilin Tang [a]*

[a] State Key Laboratory of Electroanalytical Chemistry, Changchun Institute of Applied Chemistry, Chinese Academy of Sciences, Changchun, Jilin 130022, People's Republic of China

[b] University of Chinese Academy of Sciences, Beijing, 100049, People's Republic of China

*Corresponding author: Tel./fax: +86-431-85262734

E-mail address: jltang@ciac.ac.cn (J. Tang)

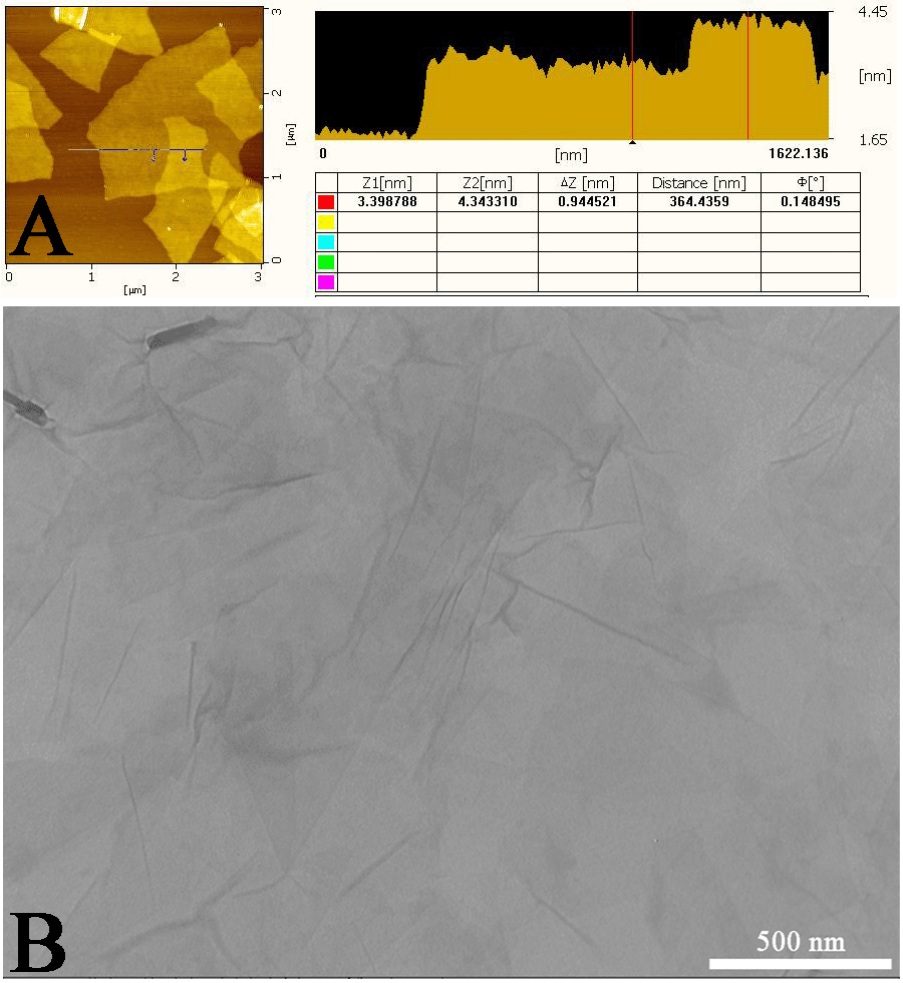

Fig. S1 AFM and TEM images of GO used for the fabrication of metal oxide-G.

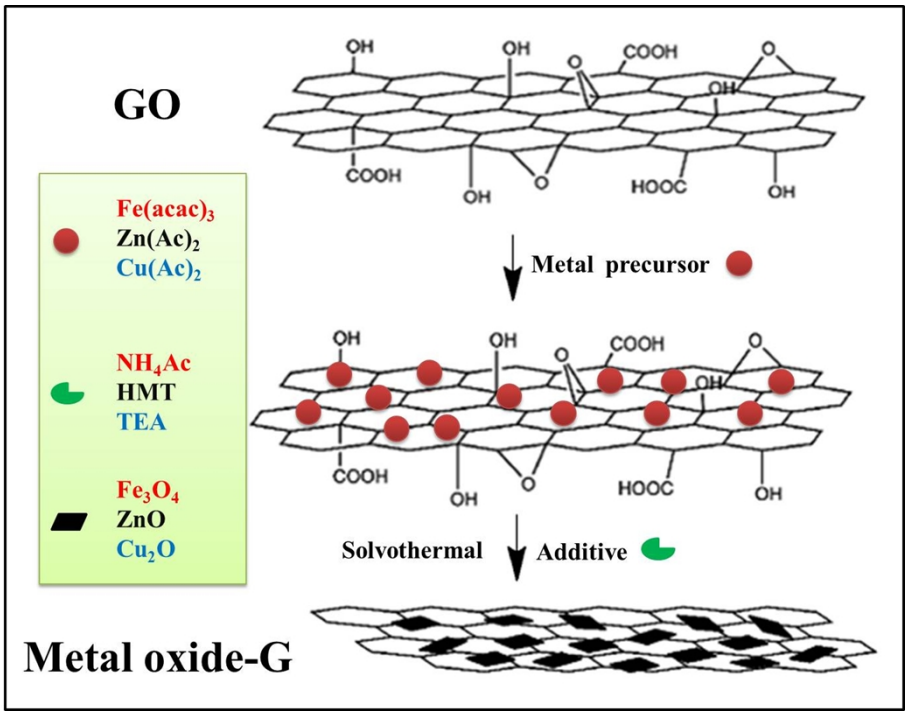

Fig. S2 Schematic illustration (not to scale) of the procedure for preparing metal oxide-G (metal oxide = Fe_3O_4, ZnO and Cu_2O) composites.

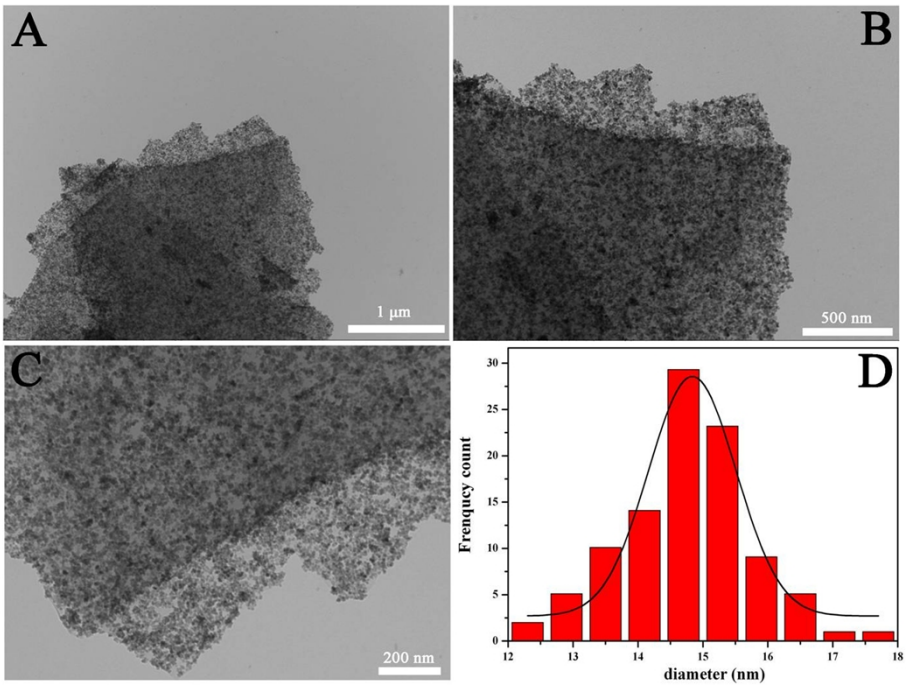

Fig. S3 TEM images with different magnification of Fe_3O_4-G (A, B and C) and the corresponding size distribution of Fe_3O_4 on the surface of graphene sheets.

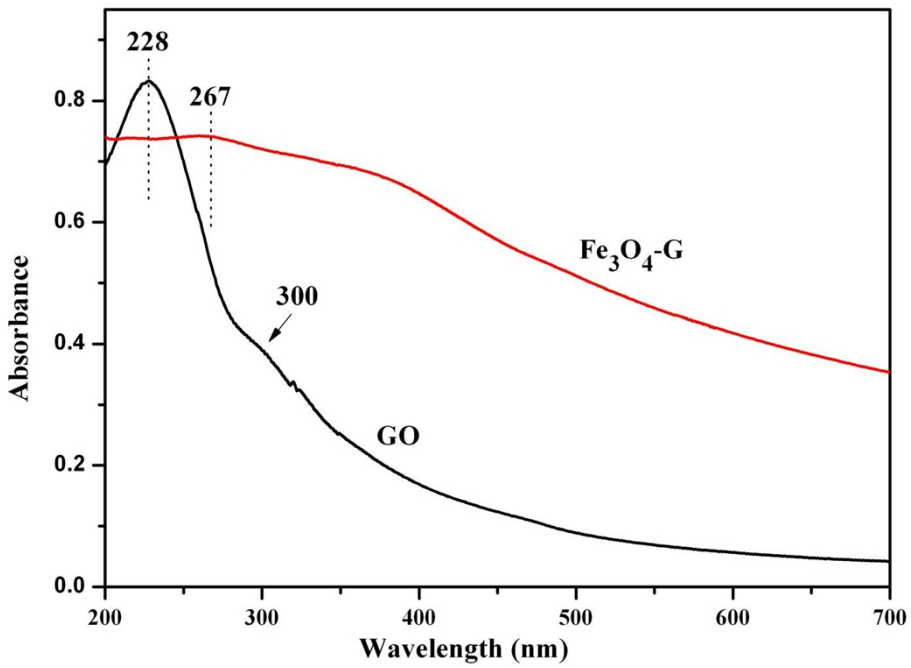

Fig. S4 UV-vis absorbance spectra of Fe_3O_4-G and GO aqueous solution.

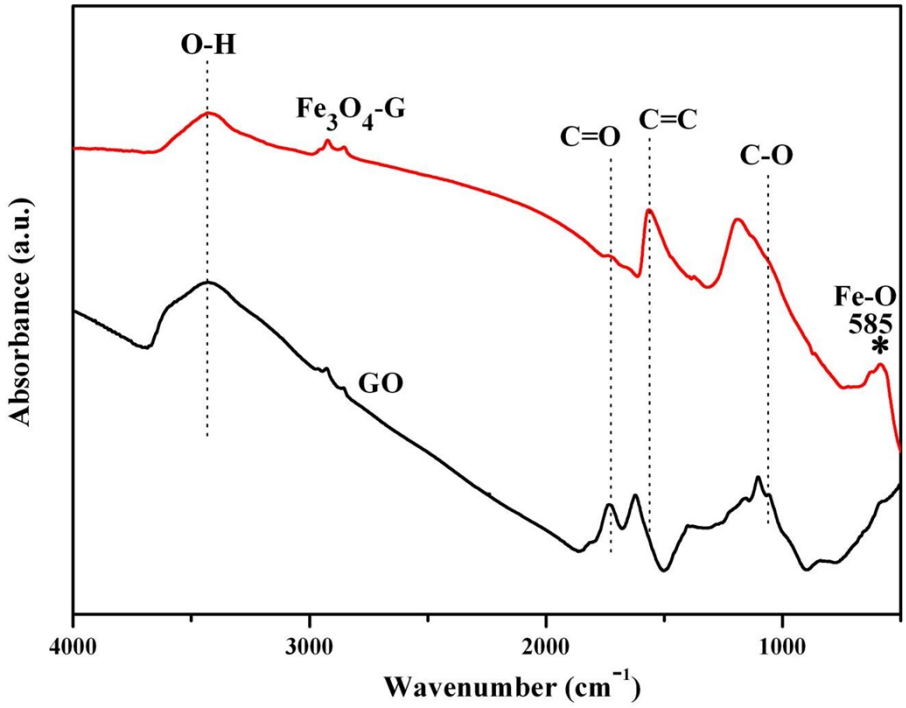

Fig. S5 FTIR spectra of Fe_3O_4-G and GO.

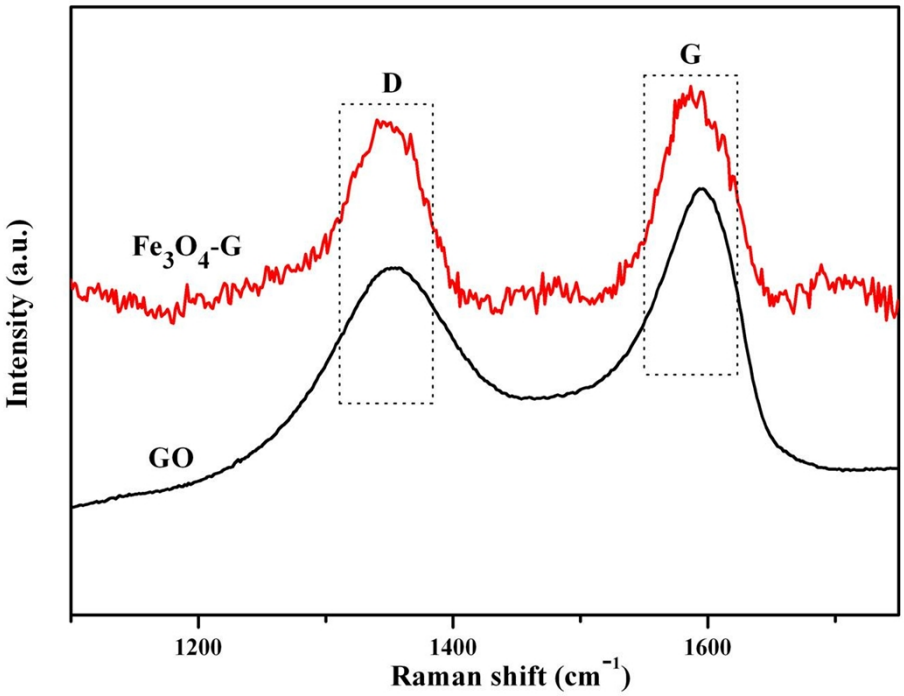

Fig. S6 Raman spectra of Fe_3O_4-G and GO.

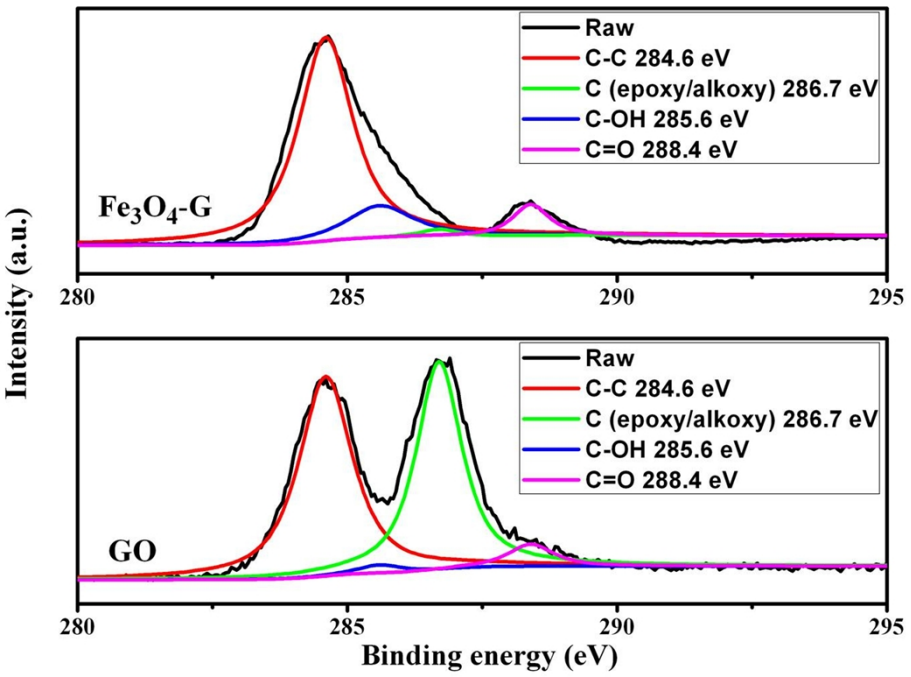

Fig. S7 High-resolution XPS spectra in the C 1s regions of Fe_3O_4-G and GO.

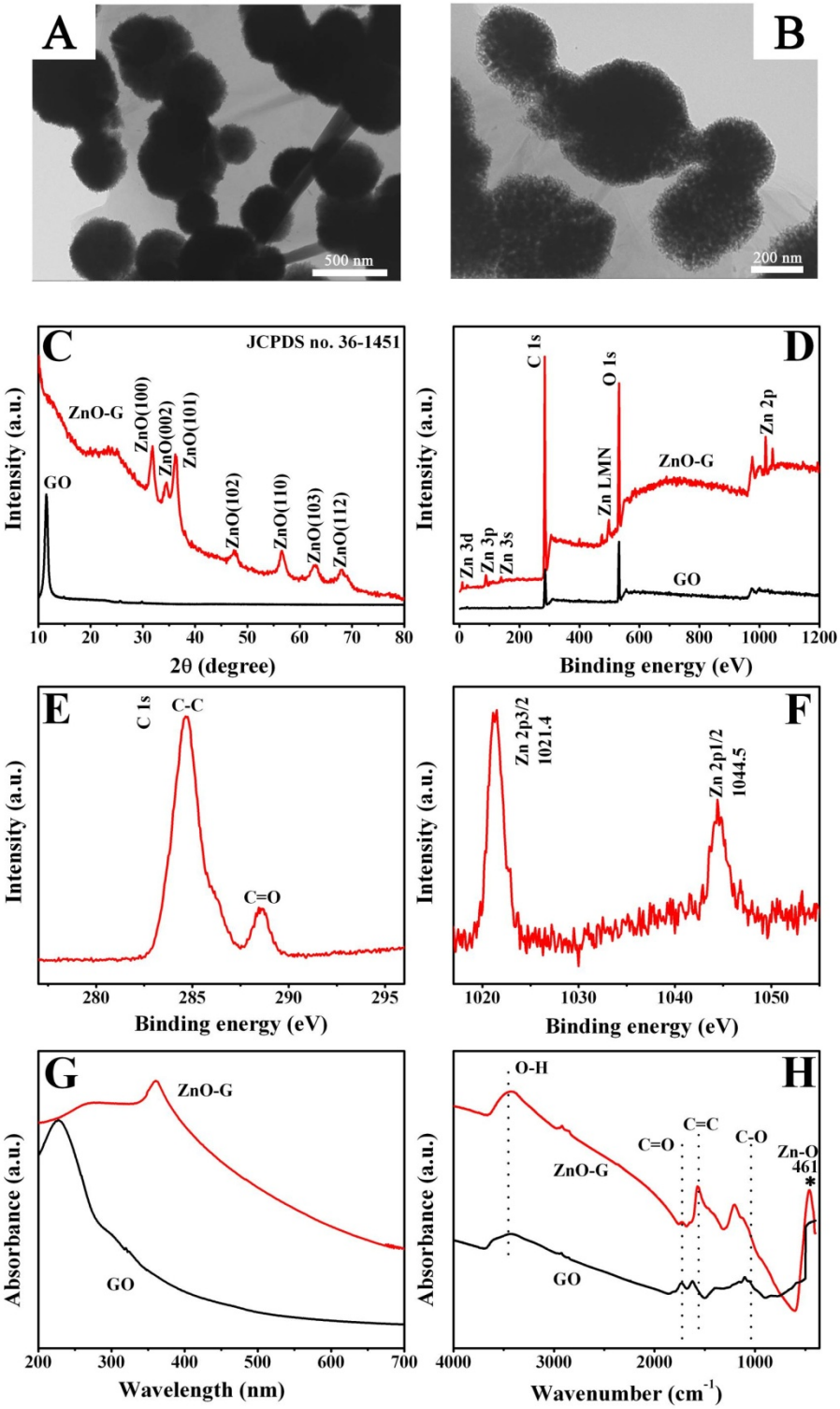

Fig. S8 TEM images of ZnO-G (A and B). XRD pattern (C) and XPS spectra (D) of ZnO-G. High-resolution XPS spectra in the C 1s (E) and Zn 2p (F) regions of ZnO-G. UV-vis absorbance spectra (G) and FTIR spectra (H) of ZnO-G.

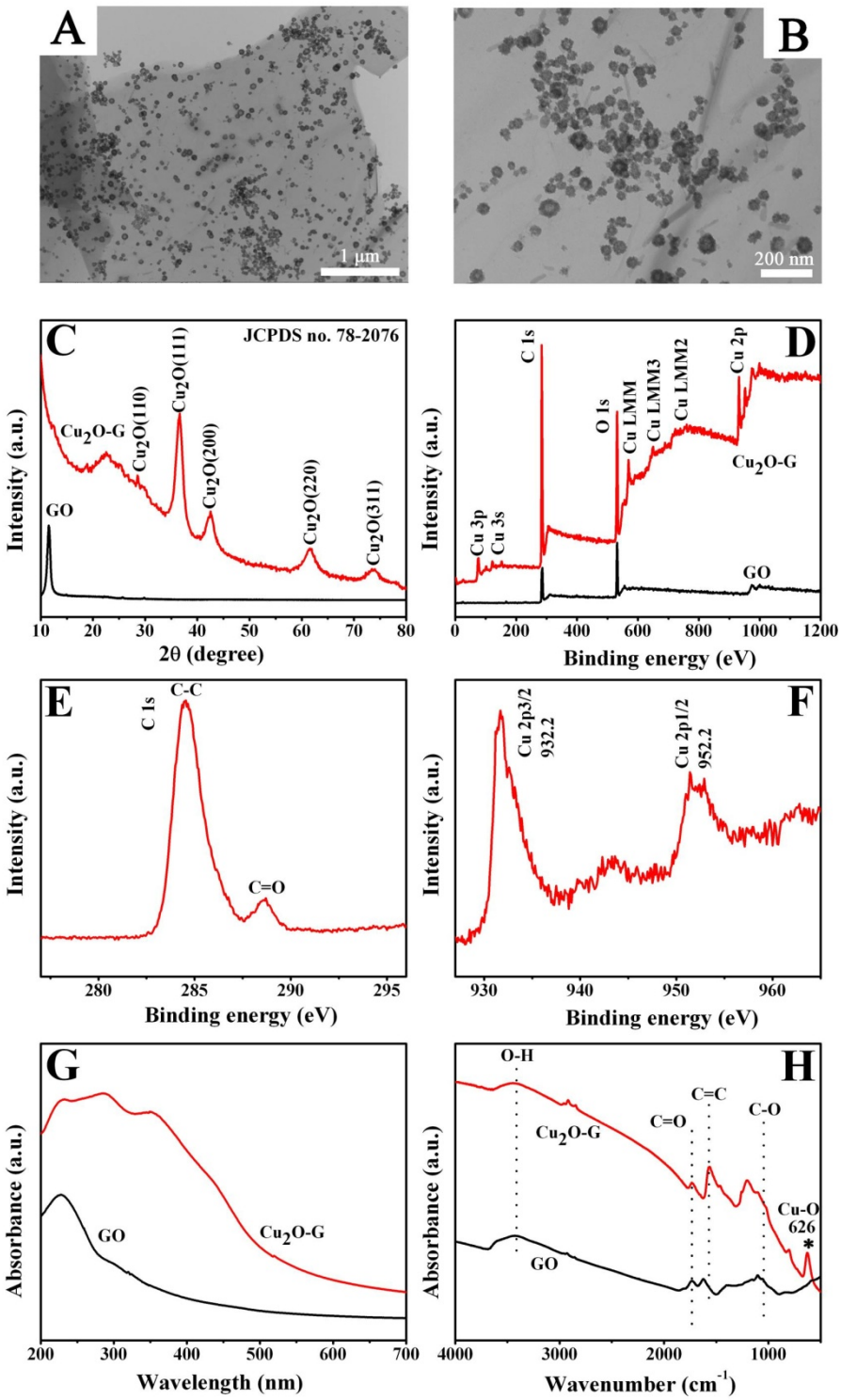

Fig. S9 TEM images of Cu_2O-G (A and B). XRD pattern (C) and XPS spectra (D) of Cu_2O-G. High-resolution XPS spectra in the C 1s (E) and Cu 2p (F) regions of Cu_2O-G. UV-vis absorbance spectra (G) and FTIR spectra (H) of Cu_2O-G.

Characterization of ZnO-G and Cu_2O-G

1. TEM characterization

The morphologies of ZnO-G and Cu_2O-G were characterized by TEM. Clearly, the stratiform G sheets covered with ZnO nanospheres or Cu_2O nanoparticles are observed, as shown in Fig. S8 (A, B) and Fig. S9 (A, B). Simultaneously, it can be seen that the ZnO and Cu_2O are predominantly located at the edges and wrinkles of G sheets, where oxygen-containing functional groups are relatively abundant, and serve as linking groups for electrostatic attraction.

2. XRD analysis

The XRD patterns of ZnO-G and Cu_2O-G are also shown in Fig. S8C and Fig. S9C. The pattern obviously consist of two sets of diffraction peaks (G and ZnO), the diffraction peak at $2\theta = 23.8^o$ correspond to G sheets and the other seven diffraction peaks correspond to wurtzite phase of ZnO, which is consistent with the standard XRD data file of ZnO (JCPDS no. 36-1451) (Fig. S8C). The pattern of Cu_2O-G also consist of two sets of diffraction peaks (G and Cu_2O), the diffraction peak at $2\theta = 22.5^o$ correspond to G sheets and the other five diffraction peaks can be indexed to cubic phase Cu_2O (JCPDS no. 78-2076) (Fig. S9C).

3. XPS of ZnO-G and Cu_2O-G

The chemical composition of ZnO-G and Cu_2O-G was obtained by XPS. The survey spectrum of ZnO-G shows the presence of Zn and O as well as C (Fig. S8D). High-resolution XPS spectra of C 1s and Zn 2p were also performed, and we can see that the XPS spectrum of C 1s can be deconvoluted into two peaks centered at 284.6 and

288.4 eV. The peak at 284.6 eV is attributed to the C=C/C–C, while the peak positioned at 288.4 eV is assigned to the O=C–OH species (Fig. S8E). The Zn 2p spectrum shows two peaks at 1021.4 and 1044.5 eV which are assigned to the 2p3/2 and 2p1/2 components, respectively, as reported for ZnO (Fig. S8F).[1] Fig. S9D is the XPS general spectra of Cu_2O-G. Apart from C and O, the element of Cu is also existed in Cu_2O-G composites. The high-resolution XPS spectrum of C 1s was shown in Fig. S9E and two peaks located at 284.6 and 288.4 eV were also observed. Besides the C 1s peak, the two peaks recorded in the region of Cu 2p at 932.2 and 952.2 eV are in agreement with the literature data for Cu_2O (Fig. S9F).[2]

4. UV-vis spectroscopy and FTIR spectra of ZnO-G and Cu_2O-G

The optical properties of ZnO-G and Cu_2O-G were investigated using UV-vis spectroscopy and FTIR. Fig. S8G was the UV-vis absorption spectra of GO and ZnO-G. Compared with GO, a sharp characteristic absorption peak at 361 nm appeared in ZnO-G, indicated the presence of good crystalline and impurity suppressed ZnO nanostructures.[3, 4] The IR spectra of GO and ZnO-G were shown in Fig. S8H. The absorption band at 461 cm^{-1} for the ZnO-G can be assigned to the stretching vibration of Zn–O.[5] The UV-vis absorption spectra and IR spectra of GO and Cu_2O-G were also shown in Fig. S9G and Fig. S9H. The Cu_2O-G nanocomposites have absorption in the whole UV-visible region ranging from 200 nm to 700 nm, similar to previously literature reported.[6] Furthermore, the IR absorption of Cu_2O-G at 626 cm^{-1} was ascribed to Cu–O bond vibration.[7]

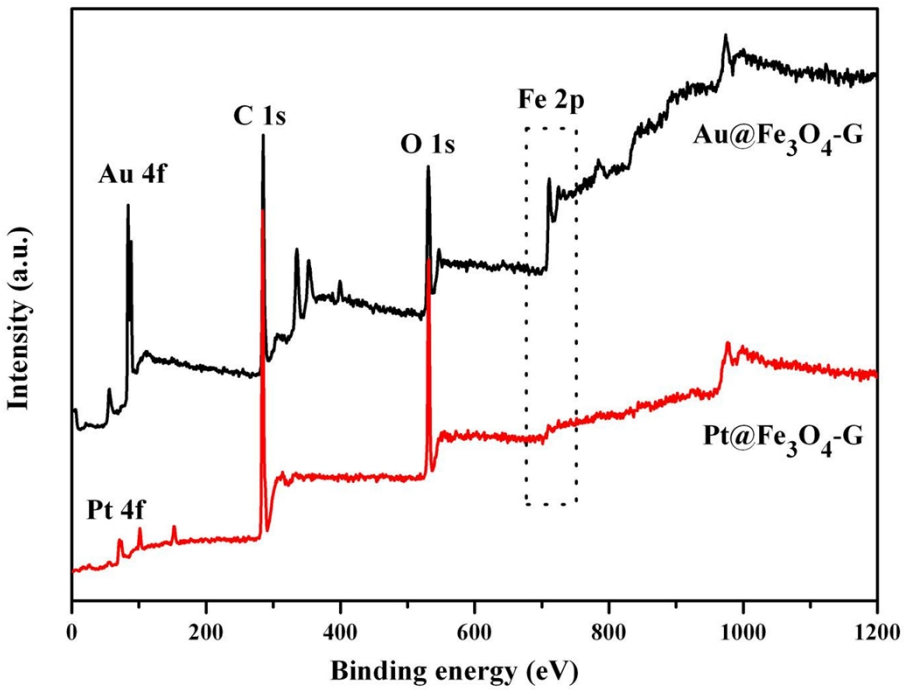

Fig. S10 XPS general spectra of Au@Fe_3O_4-G and Pt@Fe_3O_4-G.

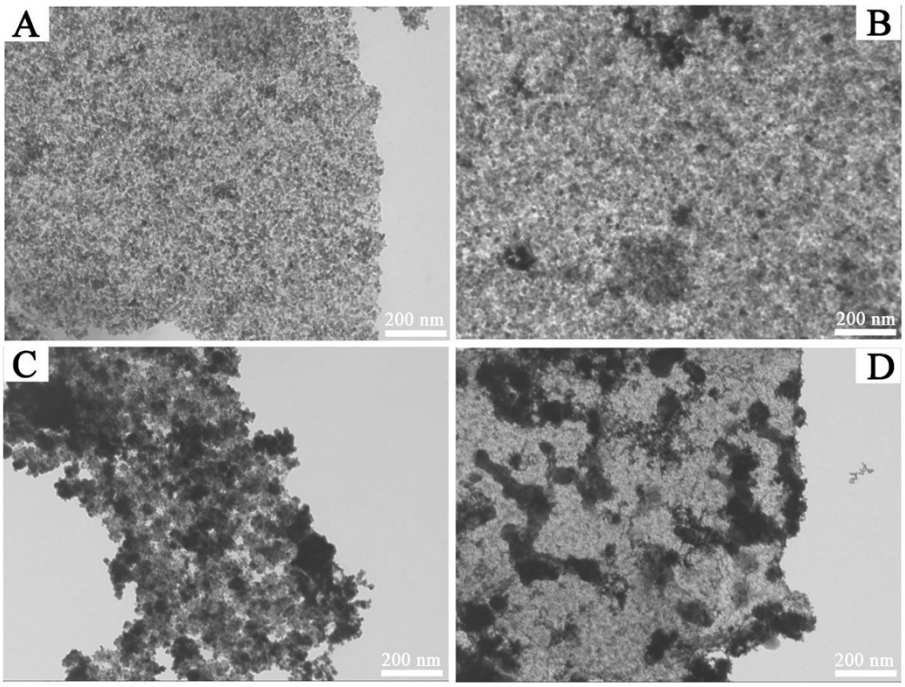

Fig. S11 TEM images of Au@Fe_3O_4-G (A, C) and Pt@Fe_3O_4-G (B, D) prepared under the same conditions except that the synthesis was conducted in the presence or absence PDDA functionalization.

Reference

1 S. Ghosh, V. S. Goudar, K. G. Padmalekha, S. V. Bhat, S. S. Indi and H. N. Vasan, *RSC Adv.* 2012, **2**, 930-940.

2 Y. Zhang, X. Wang, L. Zeng, S. Song and D. Liu, *Dalton Trans.* 2012, **41**, 4316-4319.

3 J. Wu, X. Shen, L. Jiang, K. Wang and K. Chen, *Appl. Surf. Sci.* 2010, **256**, 2826-2830.

4 F. Liu, Y. Zhang, J. Yu, S. Wang, S. Ge and X. Song, *Biosens. Bioelectron.* 2014, **51**, 413-420.

5 Y. Liu, Y. Hu, M. Zhou, H. Qian and X. Hu, *Appl. Catal., B* 2012, **125**, 425-431.

6 B. Li, T. Liu, L. Hu and Y. Wang, *J. Phys. Chem. Solids* 2013, **74**, 635-640.

7 B. Li, H. Cao, G. Yin, Y. Lu and J. Yin, *J. Mater. Chem.* 2011, **21**, 10645-10648.